In: Nonlinear Economic Dynamics ISBN 978-1-61668-788-5
Editors: Tonu Puu, Anastesiia Panchuk, pp. 43-57

Chapter 4

INTRICATE ASSET PRICE DYNAMICS AND ONE-DIMENSIONAL DISCONTINUOUS MAPS

F. Tramontana, L. Gardini and F. Westerhoff*
Department of Economics and Quantitative Methods, University of Urbino, Via Saffi 42, 61029 Urbino, Italy
Department of Economics, University of Bamberg, Feldkirchenstrasse 21, 96045 Bamberg, Germany

Abstract

In this chapter we consider a simple financial market model following the pioneering works by R. Day, described by one-dimensional piecewise linear maps, either being continuous or discontinuous. We shall see how rich the related dynamics are, with sequences of stable cycles and chaotic intervals. Our results explain, among other things, the emergence of intricate bull and bear markets dynamics, as observed in many actual financial markets. Due to its simplicity, the model allows both a useful analytical study and a qualitative interpretation of the dynamic outcomes. We describe bifurcation sequences with both period increment by one and by two, and we illustrate the wide regions of chaotic behavior.

4.1 Introduction

In this chapter we are interested in a piecewise linear model, in the case of both continuous and discontinuous maps, which comes from the study of financial markets where heterogeneous speculators follow simple technical and fundamental trading rules to determine their

* f.tramontana@univpm.it, laura.gardini@uniurb.it, frank.westerhoff@uni-bamberg.de

orders. As we will see, our model is able to generate complex dynamics. For instance, asset prices can be highly volatile and display irregular switches between bull and bear markets, as also studied recently in [1] and [2]. Inspired by the seminal papers by R. Day ([3, 4]), such simple deterministic models are still sufficiently up-to-date to interpret the current financial crises.

The financial market model we discuss in this chapter goes back to [5]. However, there are so many possible scenarios associated with that particular piecewise linear model that it is impossible to investigate all of the results in one contribution. In [5], we focused on cases in which the two linear pieces of the map have either positive or negative slopes. Now we focus on the case in which the right branch of the map has a negative slope while left has a positive slope. However, both branches have positive offsets. Due to the assumptions about the shape of the map, there is only one equilibrium, located on the right part of the map. It always exists, and can be stable or unstable. If it is unstable, however, the global dynamics are nevertheless bounded: we observe cyclical or chaotic motion, and the trajectory flips back and forth between the left and the right side of the map.

The main point in the analysis of non-smooth systems (continuous and discontinuous) is the occurrence of *border collision bifurcations* (BCB), due to the merging (or collapse) of some invariant set (a fixed point, a periodic point of a cycle, or the boundary of any invariant set) with the kink point at which the function changes its definition. This may lead to a drastic change, unexpected (i.e. impossible) in the framework of smooth systems. Such border collision bifurcations (the term was coined by Nusse and Yorke in 1992 [6], (see also [7]) are responsible, for example, for the direct transition from a regular regime to chaotic dynamics, or even to divergence ([8–11]). It is not an easy task to analyze the effect of a collision of an invariant set with a kink point, a boundary for the map definition. It is, in effect, a global bifurcation that depends on the shape of the map on "the other side" of the collision, and may lead to several different dynamic effects. For example, the dynamics can suddenly change from an attracting fixed point to an attracting cycle of any period, or to chaotic dynamics, and true chaos or strict chaos in the sense of [12], and especially robust chaos [13], since it is persistent as a function of the parameters.

The chapter is organized as follows. The model is introduced in Section 2. In Section 3 we describe some of the model's properties, including the degeneracy of all the flip bifurcations of any cycle occurring in the model under our assumptions. In Section 4 we determine the BCB curves associated with the periodicity regions of cycles with the symbol sequence L^kR and the related curves at which their degenerate flip bifurcation occurs. In Section 5 we determine the BCB curves associated with the periodicity regions of cycles with the symbol sequence LR^k, which are paired with overlapping portions. Section 6 concludes the chapter.

4.2 A Simple Piecewise Linear Financial Model

In this section, we briefly recall the financial market model proposed in [5] and clarify the economic meaning of our underlying parameter setting. We refer the reader to [5] for more empirical evidence and theoretical justification for our behavioral model as well as for related literature on agent-based models and general properties of asset price dynamics, the so-called stylized facts.

Let us start with the derivation of the model, which contains five types of agents: a market maker, two types of chartists and two types of fundamentalists. The market maker adjusts prices with respect to excess demand in the usual way. The log of price P for period $t+1$ is

$$P_{t+1} = P_t + a(D_t^{C,1} + D_t^{C,2} + D_t^{F,1} + D_t^{F,2}), \tag{4.1}$$

where a is a positive price adjustment parameter, $D_t^{C,1}$ and $D_t^{C,2}$ are the orders of the two types of chartists, and $D_t^{F,1}$ and $D_t^{F,2}$ are the orders of the two types of fundamentalists, respectively. Any positive (negative) excess demand, given by the four terms in brackets, leads to a price increase (decrease). Without loss of generality, we assume $a = 1$.

Chartists believe in the persistence of bull and bear markets. The orders of type 1 chartists are formalized as

$$D_t^{C,1} = \begin{cases} +c^{1,a}(P_t - F) & if \quad P_t - F > 0 \\ +c^{1,b}(P_t - F) & if \quad P_t - F < 0 \end{cases}, \tag{4.2}$$

where $c^{1,a}$ and $c^{1,b}$ are positive reaction parameters and F is the log of the fundamental value. Accordingly, type 1 chartists optimistically (pessimistically) buy (sell) assets when prices are above (below) the fundamental value. The orders placed by type 2 chartists are captured by

$$D_t^{C,2} = \begin{cases} +c^{2,a} & if \quad P_t - F > 0 \\ +c^{2,b} & if \quad P_t - F < 0 \end{cases}. \tag{4.3}$$

In a bull market, their buying orders amount to $c^{2,a} > 0$ while in a bear market, their selling orders total $c^{2,b} > 0$.

Fundamentalists bet on a convergence between prices and fundamental values. The orders placed by type 1 fundamentalists are expressed as

$$D_t^{F,1} = \begin{cases} +f^{1,a}(F - P_t) & if \quad F - P_t > 0 \\ +f^{1,b}(F - P_t) & if \quad F - P_t < 0 \end{cases}, \tag{4.4}$$

while the orders placed by type 2 fundamentalists are denoted by

$$D_t^{F,2} = \begin{cases} +f^{2,a} & if \quad F - P_t > 0 \\ +f^{2,b} & if \quad F - P_t < 0 \end{cases}. \tag{4.5}$$

The reaction parameters $f^{1,a}$, $f^{1,b}$, $f^{2,a}$ and $f^{2,b}$ are all positive. Note that both types of fundamentalists submit buying (selling) orders when the market is undervalued (overvalued).

Apparently, one key characteristic (and novel) feature of this framework is that type 2 agents always trade fixed amounts of assets while type 1 agents increase their orders linearly with the observed mispricing. Moreover, the agents' trading intensity depends on whether the market is in a bull or a bear state. Eight parameters are therefore required to describe the behavior of the four different groups of speculators.

Nevertheless, the model's dynamical system can conveniently be expressed using the following definitions: $s_R = 1 + c^{1,a} - f^{1,b}$, $s_L = 1 + c^{1,b} - f^{1,a}$, $m_R = c^{2,a} - f^{2,b}$ and $m_L =$

$f^{2,a} - c^{2,b}$. Combining (4.1)–(4.5) and expressing the model in terms of deviations from fundamental values, $\widetilde{P}_t = P_t - F$, yields the discontinuous one-dimensional map

$$\widetilde{P}_{t+1} = \begin{cases} s_R \widetilde{P}_t + m_R & if \quad \widetilde{P}_t > 0 \\ s_L \widetilde{P}_t + m_L & if \quad \widetilde{P}_t < 0 \end{cases} . \tag{4.6}$$

Moreover, by using $x' = \widetilde{P}_{t+1}$ and $x = \widetilde{P}_t$, the following is finally obtained:

$$x' = T(x) = \begin{cases} f_L(x) = s_L x + m_L & if \quad x < 0 \\ f_R(x) = s_R x + m_R & if \quad x > 0 \end{cases} , \tag{4.7}$$

which comprises a family of piecewise linear maps.

Of course, the dynamics of (4.7) depend on the size of the four (aggregated) slope and offset parameters. There are a number of interesting scenarios, a few of which have already been covered in [5]. However, there is no empirical evidence on the size of these parameters and thus it is worthwhile (and fascinating) to study more of them. The main focus of this chapter is on $s_R < 0 < s_L < 1$. Accordingly, in the bear market the aggressiveness of type 1 fundamentalists is "slightly" higher than the aggressiveness of type 1 chartists (such that $0 < s_L < 1$), while in the bull market it is "much" higher (and such that $s_R < 0$). Moreover, $m_L > 0$ and $m_R > 0$ mean that type 2 fundamentalists dominate type 2 chartists in the bear market, and vice versa in the bull market. Note also that $m_L > m_R$ indicates that the dominance of type 2 fundamentalists over type 2 chartists in the bear market may be regarded as larger than the dominance of type 2 chartists over type 2 fundamentalists in the bull market. Of course, $m_L < m_R$ implies the opposite. As will be pointed out in more detail in Section 3, we additionally require in the latter case that the distance between m_L and m_R, and thus the "difference in dominance", is limited, i.e. we assume that $m_L \geq x_R^*$, where $x_R^* = m_R/(1 - s_R)$ is the unique fixed point of the model.

To be able to appreciate our results, let us also put these new cases into perspective with the two (main) cases explored so far. In [5] we analyzed scenarios in which type 1 chartists are always dominated by type 1 fundamentalists while simultaneously type 2 chartists always dominate type 2 fundamentalists (or the other way around). In this contribution, we depart from this kind of symmetry; now, a dominance of one trader type over the other and the level of dominance may depend on economic circumstances, that is, whether the market is in a bear or a bull state. It is interesting to investigate how the departure from this kind of symmetry may affect the dynamics of the model. Is such a twist sufficient to destroy the model's potential to generate complex endogenous price dynamics? As we will see, the opposite holds. Our analysis illustrates that the corresponding map still gives rise to intricate (price) dynamics and thus that the results derived in [5] may be regarded as robust.

4.3 Some Properties of the Model

The family of maps we consider is given in (4.7). The restrictions on the parameters we impose in this chapter are:

$$s_R < 0 < s_L < 1 \ , \ m_L \gtreqless m_R \ , \ m_{L,R} > 0 \tag{4.8}$$

so that we have an increasing straight line for $x < 0$ and a decreasing straight line for $x > 0$. The shape of the map (4.7) is shown in Fig. 4.1a,b.

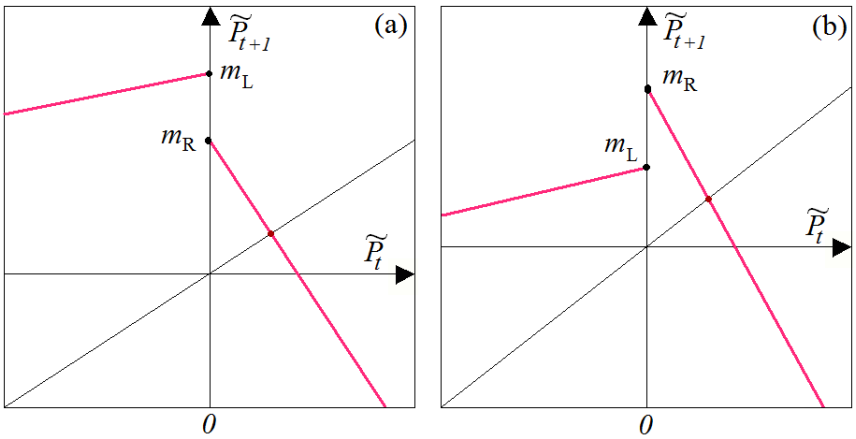

Figure 4.1: The two cases under analysis.

Hence, since we limit the branch on the left to a positive slope and less than one, we have no equilibrium on the left, and the iterated points are pushed to the right, where a negative slope exists. In case of an unstable fixed point, the generic trajectory is necessarily forced to return (after a finite number of turns around the unstable fixed point) to the left, where an increasing sequence will start again. Thus the dynamics are always bounded in a natural way: they can never explode (diverge). The different regimes which can occur under (4.7) and (4.8) are visualized in Fig. 4.1a,b from which we can conclude that:

(i) either the left branch ends above the right one, $m_L \geq m_R$ (as in Fig. 4.1a), and the map is continuous in the case of $m_L = m_R$ and discontinuous otherwise;

(ii) or the left branch ends below the right one, yet remains above the fixed point $x_R^* \leq m_L < m_R$ (as in Fig. 4.1b);

(iii) or the left branch ends below the fixed point, $0 < m_L < x_R^* (< m_R)$.

To keep this chapter concise, we limit our analysis to cases (i) and (ii). As we shall see, the dynamics occurring in the continuous case are the same as those which may occur for a decreasing jump when $m_L > m_R$. That is, the continuous case can only be considered a particular one in class (i) given above. Hence, since our results are totally generic and depend on all of the parameters of the model, the equations giving the border collision bifurcation curves and the flip bifurcations curves of the cycles occurring in the continuous case are the same as those detected for the discontinuous case, with the particular choice of parameters $m_L = m_R$.

Due to the simplicity of the model, it is quite easy to determine the eigenvalue associated with a certain cycle. In fact, a periodic orbit with period $k = p + q$ with p points on the L side and q points on the R side, necessarily has eigenvalue $\lambda = s_L^p s_R^q$. Moreover, we shall see that the cases (i) and (ii) defined above, all of the cycles that may be stable necessarily have a negative eigenvalue, so that they can only have a bifurcation with eigenvalue $\lambda = -1$, which in our piecewise linear map is always a degenerate flip bifurcation. A degenerate flip bifurcation of a k-cycle is such that at the bifurcation value (when the eigenvalue is equal

to -1), the map possesses an interval filled with cycles of period $2k$ (with the $k-$cycle in between). This is also a border collision bifurcation (for the cycle at the boundary of the interval), meaning that it is generally not known what occurs after a degenerate flip bifurcation. In our model, the degenerate flip bifurcation of the fixed point is followed by a unique stable $2k-$cycle in case (i), and by chaotic dynamics in case (ii).

Let us start with the equilibrium of our model: the fixed point that comes from the function on the right side. From $f_R(x_R^*) = x_R^*$, a fixed point $x_R^* > 0$ is given by:

$$x_R^* = \frac{m_R}{1 - s_R} \tag{4.9}$$

which is attracting for $-1 < s_R < 0$. A degenerate flip bifurcation occurs when $s_R = -1$, which means that at the bifurcation value all of the points of interval I :

$$I = [{f_R}^2(0), f_R(0)] = [0, m_R] \tag{4.10}$$

are cycles of period 2 (except for the fixed point). After the bifurcation, only one cycle of period 2 may or may not be left. A $2-$cycle must necessarily be of symbol sequence LR. The two periodic points can be easily found, solving for $f_L \circ f_R(x) = x$, which gives the periodic point on the R side, and solving for $f_R \circ f_L(x) = x$, which gives the periodic point on the L side, so that we obtain

$$x_0 = \frac{s_R m_L + m_R}{1 - s_L s_R} < 0 \ , \ x_1 = \frac{s_L m_R + m_L}{1 - s_L s_R} > 0 \tag{4.11}$$

which, when existing, is stable for $-1 < \lambda_2 = s_R s_L < 0$. Its existence is associated with the condition given by the numerator of x_0 (as the denominators are always positive), that is: $s_R < -\frac{m_R}{m_L}$ and the border collision bifurcation leading to its existence is $s_R = -\frac{m_R}{m_L}$ yielding $x_0 = 0$, while the second possible border collision bifurcation associated with $x_1 = 0$ can never occur (since under our assumptions on the parameters we always have $(s_L m_R + m_L) > 0$.

We can therefore immediately see that in the continuous case, when $m_L = m_R$, the BCB of the $2-$cycle reduces to $s_R = -1$ and thus corresponds to the degenerate flip bifurcation of fixed point x_R^*. While in the discontinuous case, when $m_L > m_R$, the BCB of the $2-$cycle is associated with a value $-1 < s_R < 0$ to which an attracting fixed point corresponds. This implies a region of coexistence of the stable fixed point with the stable $2-$cycle (born by border collision bifurcation). Thus, keeping the values of parameters m_L and m_R fixed, a $2-$cycle will be left at the degenerate flip bifurcation of the fixed point, attracting if $-1 < \lambda_2 = s_R s_L < 0$ or repelling if $s_R s_L < -1$. However, in our assumptions $(0 < s_L < 1)$ for $m_L > m_R$ only a stable $2-$cycle can occur.

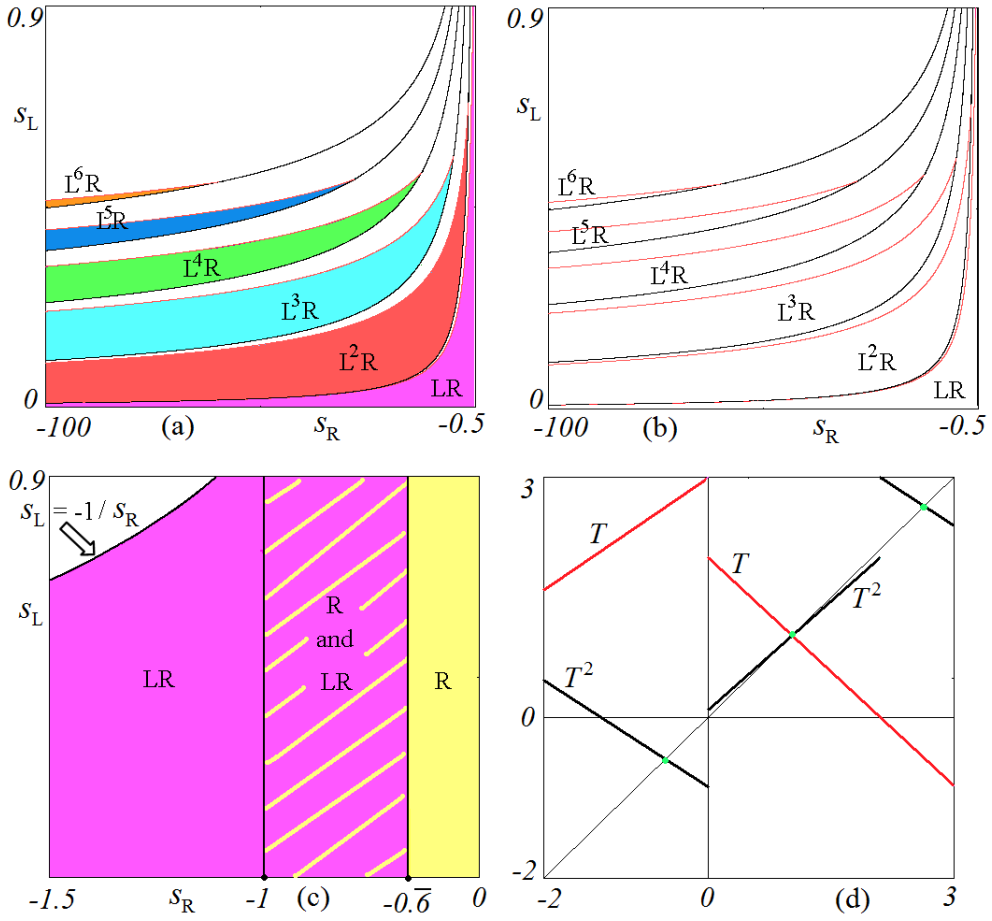

Figure 4.2: Two dimensional (s_R, s_L) bifurcation diagram in (a) and related BCB curves in (b), at $m_L = 3$ and $m_R = 2$. The enlarged portion for $-1.5 < s_R < 0$ is shown in (c) where the coexistence region occurs for $-1 < s_R < -m_R/m_L = 0.\overline{6}$. In (d) the shape of the map and of its second iterate are presented.

In Fig. 4.2a we represent the generic shape of the two-dimensional bifurcation diagram in the slopes (s_R, s_L) for $m_L \geq m_R$ and an enlarged portion in Fig. 4.2c shows the region of coexistence of the stable fixed point with the stable $2-$cycle. The shape of the map T and of its second iterate T^2 in this region is shown in Fig. 4.2d for $m_L = 3 > m_R = 2$, $s_R = -0.95$ (so that the fixed point is stable), and $s_L = 0.7$. When these two periodic orbits coexist, the basin of attraction of the fixed point x_R^* is bounded by the discontinuity point and its rank-1 preimage on the right side, i.e. $\mathcal{B}(x_R^*) =]0, -m_R/s_R[$, while the other real initial conditions converge to the $2-$cycle. Note also that defining $T(0) = m_L$ this point converges to the $2-$cycle while defining $T(0) = m_R$ this point converges to the stable fixed point.

On the other hand in the discontinuous case with $m_L < m_R$, the BCB of the $2-$cycle is associated with a value $s_R = -\frac{m_R}{m_L} < -1$, so that when the flip bifurcation of the fixed point occurs (at $s_R = -1$), a $2-$cycle cannot exist and, the behavior is complex, as we can argue from the bifurcation diagram in Fig. 4.3.

As stated above, our results are generally valid regardless of the value of the parameters,

under the restriction given in (4.8). In order to simplify the exposition, our figures are related to a fixed value $m_R = 2$, which can be any positive value, and $m_L = 3$, $m_L = 1$, which can be substituted with any value $m_L \geq m_R$, $x_R^* \leq m_L < m_R$, respectively. The same qualitative figures and bifurcations are obtained, as described in the following sections, where we shall analyze what kind of dynamics occur in the model when fixed point x_R^* is unstable, and in particular the structure of chaotic trajectories.

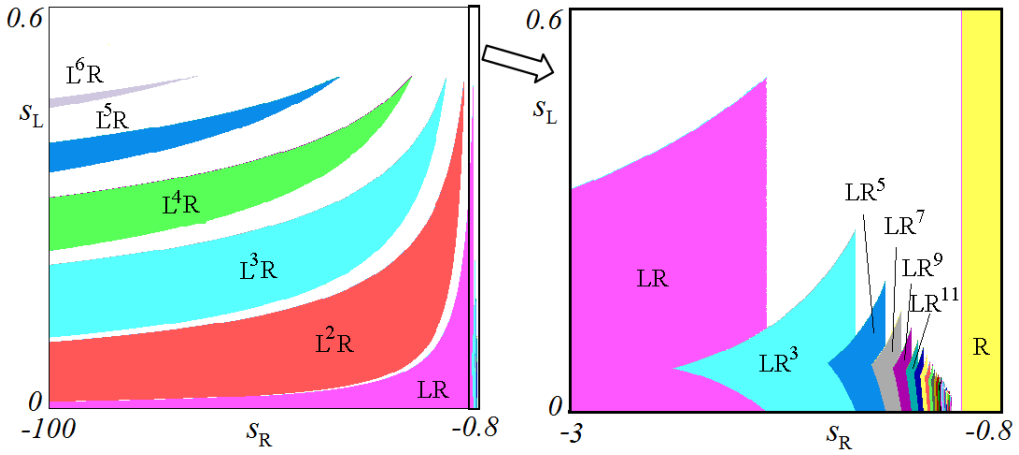

Figure 4.3: Two-dimensional orbit diagram at $m_L = 1$ and $m_R = 2$.

Fig. 4.3 represents the generic shape of the two-dimensional bifurcation diagram in slopes (s_R, s_L) in case (ii), when $x_R^* \leq m_L < m_R$. We can see that there are two typical scenarios. An increasing sequence of periodicity regions of $k-$cycles for any integer $k = 1, 2, 3, \ldots$, described in Section 4 (of type L^kR, with period increment by 1). In the enlargement between the periodicity region of the fixed point on the R side, x_R^*, and the periodicity region of the $2-$cycle, there is an infinite sequence of periodicity regions of stable $2p-$cycles, of even periods only, which we call period increment, with increment 2 (of type LR^k, with period increment by 2), as described in Section 5.

In case (i), when $m_L \geq m_R$, as shown in Fig. 4.2a, the region of (coexistence) of the stable fixed point leads directly to a stable $2-$cycle, and for low values of the slope s_R only stable cycles of type L^kR, with period increment 1, exist.

The white regions in Fig. 4.2a and Fig. 4.3a represent parameter combinations at which chaotic dynamics occur, thus in both cases wide parameter regions with chaos exist. The chaotic regime in these kinds of maps is associated with *cyclical chaotic intervals*, and chaos is called *robust* (see [13]) because it is persistent with respect to parameter variations. Although the different kinds of cyclical chaotic intervals occurring in our model are not investigated in this chapter, we shall note a peculiarity: the underlying structure associated with the unstable cycles of period L^kR also influences the chaotic trajectories. We provide some typical numerical examples in the following sections.

4.4 Maximal Cycles L^kR

In this Section we describe the BCB curves involved in the period increment scenario where the period increases by one. Let us call x_0 the point of the cycle immediately to the left of the discontinuity point $x = 0$. Then the periodic point x_0 of the orbit of symbol sequence L^kR can be obtained by looking for the fixed point of the function ${f_L}^{k-1} \circ f_R \circ f_L(x)$, that is, by solving for ${f_L}^{k-1} \circ f_R \circ f_L(x) = x$, where the 2−cycle is obtained again for $k = 1$. We have:

$$ {f_L}^{k-1} \circ f_R \circ f_L(x) = s_L^k s_R x + s_L^{k-1}(s_R m_L + m_R) + m_L \frac{1 - s_L^{k-1}}{1 - s_L} $$

so that we get:

$$ x_0 = \frac{s_L^{k-1}}{1 - s_L^k s_R}[(s_R m_L + m_R) + m_L \phi_{k-1}^L] \ , \ \phi_k^L = \frac{1 - s_L^k}{(1 - s_L)s_L^k} \tag{4.12} $$

and setting $x_0 = 0$, we obtain the BCB curve of equation:

$$ BCB_{L^kR} \ : \ s_R = -\phi_{k-1}^L - \frac{m_R}{m_L} \tag{4.13} $$

which bounds the existence region of these cycles of period $(k+1)$, given by $s_R < -\phi_{k-1}^L - \frac{m_R}{m_L}$. Moreover, it is a complete existent region. It cannot be followed by a second BCB curve leading to the disappearance of the cycle because, as we have seen for the cycle of period 2, we always have $x_1 = f_L(x_0) > 0$ for any such cycle, so that it can never merge with the boundary $x = 0$. It follows that it can only be attracting or repelling before or after the degenerate flip bifurcation occurs, when its eigenvalue $\lambda(L^kR) = s_L^k s_R$ bifurcates. Thus the equation of the flip bifurcation curve of an existent $(k+1)$−cycle is given by $\lambda(L^kR) = s_L^k s_R = -1$, that is:

$$ s_R = -1/s_L^k \tag{4.14} $$

For increasing values of k, up to 6, the BCB curves given in (4.13) are drawn in black in Fig. 4.2b, while the flip bifurcation curves given in (4.14) are drawn in red.

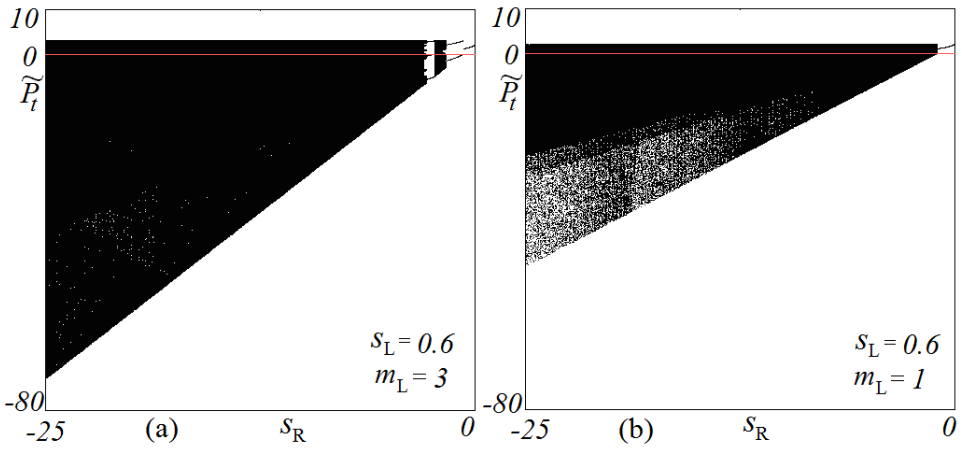

Figure 4.4: Bifurcation diagrams.

Figs. 4a and 5a show a one-dimensional bifurcation diagram at $s_L = 0.6$ and $s_L = 0.4$, respectively, in case (i), while Figs. 4b and 5b show the analogous situation for case (ii). As we can see, the degenerate flip bifurcations occurring in Fig. 4.5 are always followed by cyclical chaotic intervals, which become a one-piece chaotic interval (after a short interval in the parameter).

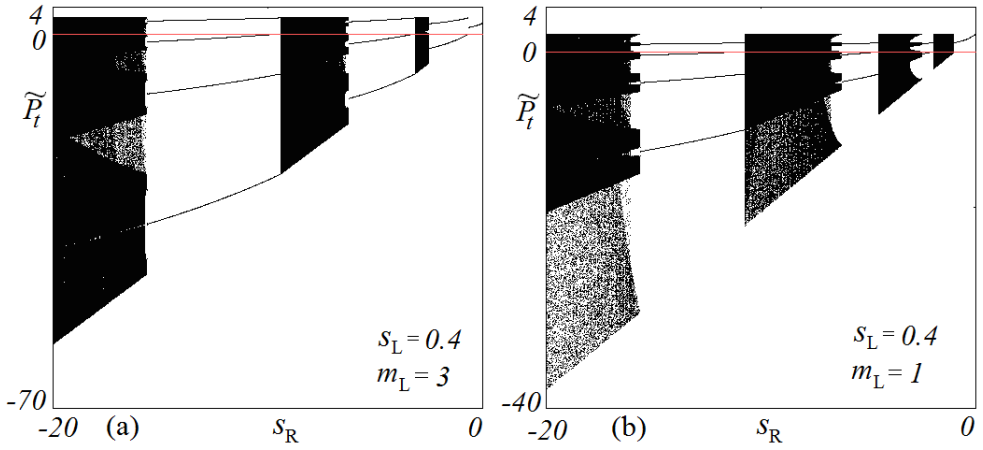

Figure 4.5: Bifurcation diagrams.

The kind of chaotic dynamics that may occur differ significantly from the usual chaotic trajectories, where we can have an unpredictable number of iterations on both sides. Here, depending on the slopes of the functions, we have always a limited number of points in each region, so that the chaotic structure is in some sense predictable, depending on the slopes. For example, we can always have only one point on the L side for small slopes of s_R in absolute value (Fig. 4.6a), or we can always have only one point on the R side for very high slopes of s_R (Fig. 4.6c), and intermediate situations otherwise (as in Fig. 4.6b).

We have described the equations of the BCB leading to the appearance of cycles with symbol sequence L^kR and have seen that a second BCB curve does not exist. This is the only possible dynamic behavior when $m_L \geq m_R$, as *when the fixed point is unstable*, the fate of point $f_R(0) = m_R$ is the same as that of $f_L(0) = m_L \geq m_R$. Hence we notice in such regimes that the definition of the map in the discontinuity point, $T(0) = m_R$ or $T(0) = m_L$, is irrelevant, as both cases lead to the same attracting set, i.e. we get the same kind of dynamics.

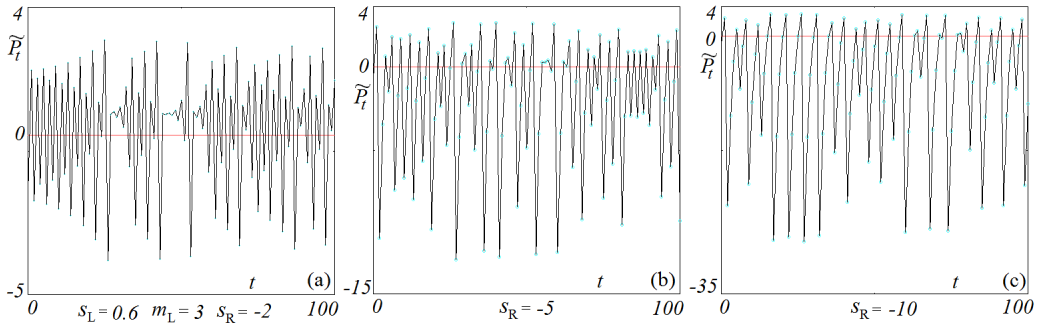

Figure 4.6: Price versus time.

This kind of dynamic behavior can also exist when $x_R^* \leq m_L < m_R$ for parameters in the left region with respect to the $2-$cycle, i.e. for $s_R \leq -\frac{m_R}{m_L}$. The price versus time trajectories in the chaotic regime are also similar, depending on the slopes. An example is given in Fig. 4.7 for $m_L = 1 < m_R$. We can always only have one point on the L side for small slopes of s_R in absolute value (Fig. 4.7a), or we can only always have one point on the R side for very high slopes of s_R (Fig. 4.7c), and intermediate situations otherwise (as in Fig. 4.7b).

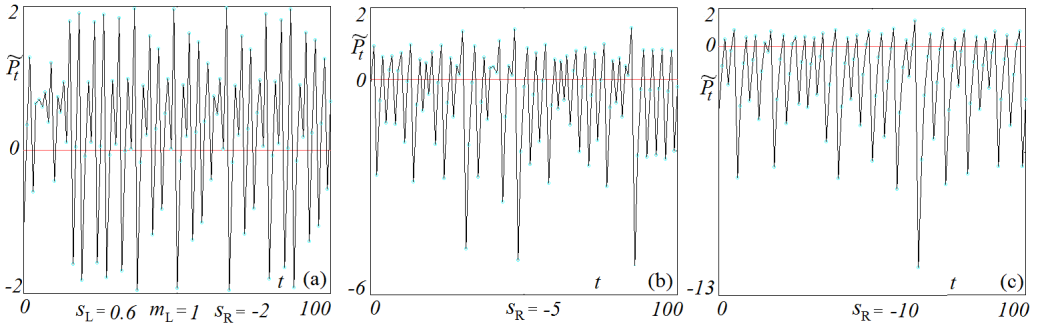

Figure 4.7: Price versus time.

While for $x_R^* \leq m_L < m_R$ and $s_R > -\frac{m_R}{m_L}$ as shown in the enlarged part of Fig. 4.3, we can have a different dynamic behavior, with periodicity regions that overlap, giving well-known regions with *two coexisting attracting cycles,* and the two different definitions of the map in the discontinuity point converge to two different cycles (with a period which differs by 2), as proved in the next section.

4.5 Maximal Cycles LR^k

As stated above, the iterations may clearly behave differently when $x_R^* \leq m_L < m_R$, as in such a case, also when the fixed point is unstable, the two points $f_L(0) = m_L$ and $f_R(0) = m_R$ may have a different dynamic behavior. This is not a new phenomenon. Indeed, when $x_R^* \leq m_L < m_R$, we can have not only cycles of the kind L^kR (when $s_R \leq -\frac{m_R}{m_L}$), but also cycles with symbol sequence LR^k (when $s_R > -\frac{m_R}{m_L}$). The reason for this is immediately clear when we look at the graph in Fig. 4.1a: point $f_L(0) = m_L$ may be much less than

m_R and close to the unstable fixed point x_R^* so that several applications of function $g(x)$ on the R side are necessary before reaching the L side. Moreover, as we shall see below, the coexistence of two stable cycles of symbol sequence LR^k and LR^{k+2} is allowed in suitable regions for any odd $k \geq 1$. To find the conditions leading to the existence of these new kinds of cycles, let us call x_0 the point of the cycle which is immediately to the left of discontinuity point $x = 0$. Then the periodic point x_0 of the orbit of symbol sequence LR^k can be obtained by looking for the fixed point of the function $f_R^k \circ f_L(x)$, that is, solving for $f_R^k \circ f_L(x) = x$. We have:

$$f_R^k \circ f_L(x) = s_R^k(s_L x + m_L) + m_R \frac{1 - s_R^k}{1 - s_R}$$

so that we obtain:

$$x_0 = \frac{s_R^k}{1 - s_R^k s_L}[m_L + m_R \phi_k^R] \quad , \quad \phi_k^R = \frac{1 - s_R^k}{(1 - s_R)s_R^k} \tag{4.15}$$

and setting $x_0 = 0$ we obtain the BCB curve of equation:

$$BCB_{LR^k}^l \quad : \quad m_L + m_R \phi_k^R = 0. \tag{4.16}$$

We denote this by $BCB_{LR^k}^l$ because at the border collision periodic point x_0 of the cycle collides with discontinuity point $x = 0$ from the left. In the parameter plane (s_R, s_L) of Fig. 4.8, such curves are vertical lines of equation $s_R = const.$, where the constant value is determined from the equations in (4.16).

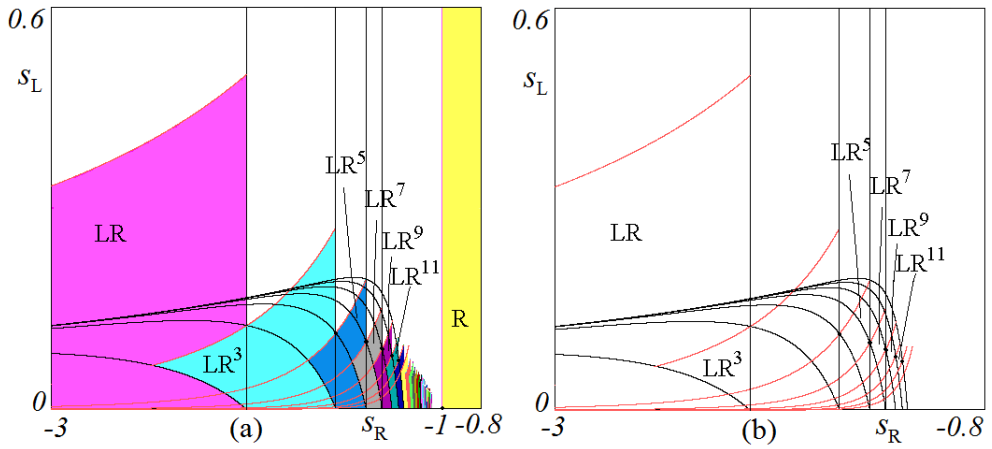

Figure 4.8: Two-dimensional orbit diagram.

We also notice that such a BCB curve $BCB_{LR^k}^l$ leads to a cycle with periodic point $x_1 = f_L(x_0) > x_R^*$. In fact by assumption, we have $f_L(0) = m_L \geq x_R^*$ at the bifurcation value and thus the existent cycle starts with periodic point $x_1 = f_L(x_0) > x_R^*$. This implies that periodic point x_1 may be mapped on the L side after an even number of applications of function $g(x)$, so that *such cycles only exist when k is an odd number,* and period $(k+1)$ is even. Moreover, it is obvious that such cycles only exist as long as another border collision

occurs, due to periodic point x_{k-1} (*which implies* $k > 1$) merging with discontinuity point $x = 0$. Equivalently, the cycle exists as long as periodic point x_k merges with the maximum value $f_R(0) = m_R$. That is to say, $x_{k-1} = 0$ iff $x_k = m_R$ iff $x_0 = f_R(m_R)$. Thus we have the equation of the second BCB curve, obtained by equation $x_0 = m_R(1+s_R)$, that is:

$$\frac{s_R^k}{1-s_R^k s_L}[m_L + m_R\phi_k^R] = m_R(1+s_R) \tag{4.17}$$

which leads to:

$$BCB^r_{LR^k} \quad : \quad s_L = \frac{1}{s_R^k} - \frac{m_L}{m_R(1+s_R)} - \frac{\phi_k^R}{(1+s_R)}. \tag{4.18}$$

We call this $BCB^r_{LR^k}$ because at the border collision periodic point x_{k-1} of the cycle collides with discontinuity point $x = 0$ from the right. A few BCB curves on both sides, from (4.16) and (4.18), are shown in black in Fig. 4.8 (the $BCB^l_{LR^k}$ are the vertical lines).

We have noticed above that such bifurcation curves $BCB^r_{LR^k}$ only exist for $k > 1$, since for $k = 1$ we have the $2-$cycle, whose periodic point x_1 can only collide the fixed point x_R^*, as already mentioned in Section 3.

We can see from Fig. 4.8a that the cycles determined here may be stable or unstable. Stability is associated with the related eigenvalue. We know this must be negative, because we have an odd number of periodic points in the R region, so that $\lambda(LR^k) = s_L s_R^k < 0$, and its flip bifurcation occurs at $\lambda(LR^k) = s_L s_R^k = -1$, that is:

$$s_L = -1/s_R^k. \tag{4.19}$$

The related flip bifurcation curves are shown in red in Fig. 4.8.

Fig. 4.8 also emphasizes that the numerically calculated flip bifurcation curves always intersect at the same point of two BCB curves. That is: each curve $BCB^l_{LR^k}$ and $BCB^r_{LR^{k+4}}$ intersects exactly at a point belonging to the flip bifurcation curve of cycle LR^{k+2}, *which proves that two stable cycles at most can coexist*. This property can be easily verified from the related equation. In fact, by using the relation

$$\phi_{k+1}^R = \phi_k^R + \frac{1}{s_R^{k+1}}$$

after some algebra it follows that $\phi_k^R = -\frac{m_L}{m_R}$ from (4.16) and $s_R^k = -\frac{1}{s_L s_R^2}$ from (4.19) for cycle LR^{k+2} identically satisfy the equation of $BCB^r_{LR^{k+4}}$.

The relevant result in this regime is that a stable cycle may not be the only existent cycle, i.e. may be not globally attracting, as we have seen that we can have a stable cycle and also several unstable cycles placed on the basin boundary of the stable one. Moreover, in particular regions we have the *coexistence of two stable cycles*.

4.6 Conclusion

In this chapter we considered a piecewise linear discontinuous map with one increasing branch on the L side and a decreasing branch on the R side, both having positive offsets,

and representing interactions between heterogeneous traders in a financial market. We determined the border collision bifurcation curves leading to the existence of stable cycles in two qualitatively different regimes for the values of the jump. In case (i), for $m_L \geq m_R$, only stable cycles of symbolic sequence L^kR can exist, whose BCB curves are given in Section 4. In case (ii), for $x_R^* \leq m_L < m_R$ there are all the stable cycles LR^k for $s_R \leq -\frac{m_R}{m_L}$. In region $-\frac{m_R}{m_L} < s_R < -1$ there are overlapping periodicity regions for stable cycles of even periods only, of type LR^k, whose BCB curves were determined in Section 5. Some regions have still not been explored, and several parameter constellations for the models considered here have been left for further studies.

Finally, let us reflect the dynamic properties of our model from an economic point of view. As is well known, actual financial markets are quite volatile, occasionally displaying severe bubbles and crashes. Our model obviously has the potential to replicate such features, at least in a qualitative manner. Besides fixed point dynamics, we also find periodic or chaotic motion (and some intriguing examples are given in Figures 6 and 7 with strongly fluctuating prices and erratic switches between bull and bear markets episodes). Moreover, there may even be coexisting attractors, and the types of bifurcations we observe imply that even a tiny shift in one of the behavioral parameters may significantly affect the variability of prices and thus the efficiency of financial markets. Given the threat originating from actual financial markets for the real economy, it is apparently very important to understand the main drivers of such dynamics. Our study ultimately illustrates that even quite simple behavioral models in which market participants follow well-established trading patterns can be useful to improve our basic understanding of what is going on in these systems.

It goes without saying that more work is required in this area. Here we studied a situation where our discontinuous map consists of two linear pieces. The next natural step would be to extend the analysis and explore models which contain three or more linear pieces.

References

[1] Tramontana, F., Gardini, L., Dieci, F., & Westerhoff, F. (2009). The emergence of "Bull and Bear" dynamics in a nonlinear 3d model of interacting markets. *Discrete Dynamics in Nature and Society*, Article ID 310471, 30 pages, doi:10.1155/2009/310471.

[2] Tramontana, F., Gardini, L., Dieci, F., & Westerhoff, F. (2009). Global bifurcations in a three dimensional financial model of "bull and bear" interactions. In C. Chiarella, G. I. Bischi & L. Gardini, (Eds.), *Nonlinear Dynamics in Economics, Finance and Social Sciences*(pp. 333–352) Springer-Verlag.

[3] Day, R. (1982). Irregular growth cycles. *The American Economic Review 72* (3), 406–414.

[4] Day, R. (1994). *Complex Economic Dynamics*. Cambridge, USA: MIT Press.

[5] Tramontana, F., Gardini, L., & Westerhoff, F. (2009). On the complicated price dynamics of a simple one-dimensional discontinuous financial market model with heterogeneous interacting traders. *submitted for publication*

[6] Nusse, H. E., & Yorke, J. A. (1992). Border-collision bifurcations including period two to period three for piecewise smooth systems. *Physica D, 57*, 39–57.

[7] Nusse, H. E., Ott, E., & Yorke, J. A. (1994). Border-collision bifurcations: An explanation for observed bifurcation phenomena. *Physical Review E, 49*, 1073–1076.

[8] Banerjee, S., Karthik, M. S., Yuan, G., & Yorke, J. A. (2000). Bifurcations in One-Dimensional Piecewise Smooth Maps - Theory and Applications in Switching Circuits. *IEEE Trans. Circuits Syst.-I: Fund. Theory Appl., 47* (3), 389–394.

[9] Maistrenko, Y. L., Maistrenko, V. L., & Chua, L. O. (1993). Cycles of chaotic intervals in a time-delayed Chua's circuit. *International Journal of Bifurcation and Chaos, 3* (6), 1557–1572.

[10] Maistrenko, Y. L., Maistrenko, V. L., Vikul, S. I., & Chua, L. O. (1995). Bifurcations of attracting cycles from time-delayed Chua's circuit. *International Journal of Bifurcation and Chaos, 5* (3), 653–671.

[11] Maistrenko, Y. L., Maistrenko, V. L., & Vikul, S. I. (1999). On period-adding sequences of attracting cycles in piecewise linear maps. *Chaos, Solitons & Fractals, 9* (1), 67–75.

[12] Day, R., & Pianigiani, G. (1991). Statistical dynamics and economics. *Journal of Economic Behavior and Organization, 16*, 37–84.

[13] Banerjee, S., Yorke, J. A., & Grebogi, C. (1998). Robust chaos. *Physical Review Letters, 80*, 3049–3052.